

Research on Designing and Manufacturing the Connecting-Rod Big End Bearing Equipment

Van Tinh Do¹, Trung Thien Pham^{*1}, Ngoc The Nguyen¹, Anh Hung Bui¹

¹University of Economic and Technical Industries, Vietnam

*Corresponding author email: pthien.ck@uneti.edu.vn

Abstract— The paper researches on designing and manufacturing system that can measure the force acting on the connecting-rod big end, thereby investigating the temperature and pressure of oil film in the it. The experimental equipment simulates the loading diagram of the internal combustion engine in 4 sessions. The connecting rod by optical elastomer material is studied by the method of using the model of connecting rod. The testing equipment can operate in a range from 0 rpm to 250 rpm. When the speed of the bearing changes, the load pattern acting on the connecting-rod big end will change, the temperature and pressure of oil film will change, too. The researching equipment in the field of lubrication and internal combustion engines can be used to verify theoretical research results and numerical simulations.

Keywords— Connecting-rod, bearing, oil film temperature. oil film pressure.

I. INTRODUCTION

From the beginning of 1969 up to now, there have been many theoretical and experimental researches on lubricating for the connecting-rod big end. These researches are divided into two main directions: theoretical research and experimental research. Theoretical research is divided into 2 main directions: static load simulation study and dynamic load simulation study. Experimental research is divided into 2 main directions: simulation of connecting rod research and real connecting rod research. Scientists around the world have started to use numerical methods to solve lubrication problems with static load bearings. In 1979, Reddy and his teammate were the first to introduce the finite element method in the study of hydrodynamic lubrication. In 2003, Stefani researched the effects of load and inertia forces on the connecting-rod big end. The study shows the pressure in the connecting rod affected by the bolt tightening force. In 2004, Stefani and Rebora researched the computational algorithms on the model of opening and sliding between the cap and the body of the connecting rod. This algorithm is used to analyze 2 or 3 dimensions of motor bearings. The cap and body of connecting rod are separated. In 2005, Fatu researched the numerical simulation and experimental lubrication of bearings under the severe working conditions. The purpose of this research was to support the designer with fast and efficient calculation tools. Viscosity changes and non-Newtonian fluids are studied in the complex cases of connecting rod big-end bearings. In 2008, Antoni and his teammates studied using a two-dimensional bearing model, consisting of two circular solids in contact with friction. The study considers the case of relative sliding between two rotating objects. In 2015, H.Shahmohamadi and his teammates studied thermal effects in large-head lubricating fluids and flow simulation solutions. Research on flow analysis with thermodynamic effects combined with Navier-Stokes solution for flow equations and energy equations.

In 2015, H. Chamani [7] research thermo-elasto-hydrodynamic (TEHD) analysis of oil film lubrication in big end bearing of a diesel engine. results of a thermoelasto-hydrodynamic (TEHD) analysis of a connecting rod big end

(BE) bearing of a heavy duty diesel engine are presented. Here, the oil film viscosity is considered a function of oil's local temperature and pressure. In 2016, H.Chamani and his teammates studied and analyzed thermodynamical elastic effects in diesel engines. The study simulates the temperature of the bearing at the speed of 1500 round/min for 3D results. Research results show that the temperature at that measurement increases significantly when the force is concentrated on the bearing. In 2017, Norbert Lorenz studied the analysis of thermal effects in hydrodynamic bearings of internal combustion engines. The author shows that the pressure and temperature of the bearing increases when the speed increases from 3000 rpm/min to 4000 rpm/min. In 2018, N.Morris and his teammates studied the effect on damage between shaft and bearing in the connecting rod on working performance. Research shows that when the shaft and bearing don't have hydrodynamic oil film, they will damage and reduce performance until they are being destroyed. The above studies show that the significance of the empirical study evaluates properly the influence of lubrication effects on the working process of the engine.

II. EXPERIENCE EQUIPMENT

A. The Sorting Bowl Design

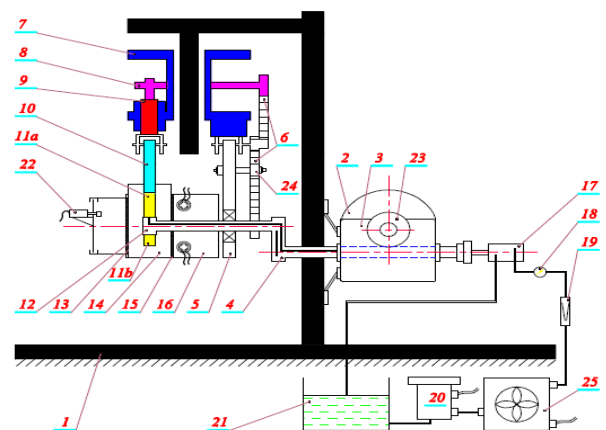


Fig. 1: Principle diagram of experience equipment

Experimental equipment for lubricating the connecting-rod big end is designed with a crankshaft- connecting rod mechanism that moves according to the crank-elbow principle and has a load that simulates the cycle of the engine. The divide consists of many mechanical structures and is presented in many topics. In this topic, the research team designs a system to measure the load acting on the connecting rod

The experimental equipment for lubricating the bearing has the principle diagram as shown in Figure 1. The electric motor(2) rotates and transmits the motion to the crankshaft(4) through the reducer and makes the crankshaft rotate. When the crankshaft rotates with the piston(7) reciprocating up and down through the steel transmission rod(5) with the shaft, the small end is fitted with the piston. This structure slides along the two pillars of the frame, the link(pillar) between the piston and the small end of the connecting rod. During working process, the connecting rod(boundary) pushes the piston up and down, this movement obeys the crank-elbow system of the heat engine. The connecting rod is placed parallel to the transmission rod. The bearing of the connecting rod big end bearing is made up of the body and cap of the connecting rod and crankshaft. The small end of the connecting rod studies the alignment and slides along the piston. During operation(when the shaft rotates), the forces generated by the piston and connecting rod movement are balanced by the pressure in the oil film of the connecting-rod big end. In order to ensure the simulation of the explosion as in a real engine, such as a 4-stroke engine more accurately, the piston is attached with a downloaded piston mechanism(9), the shaft (8) is driven by pulley and belt(6).

B. The loading structure

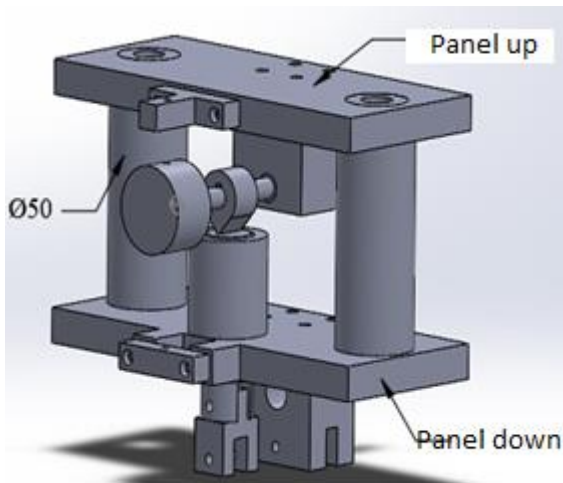


Fig. 2: The loading structure

The cam generates compression when the top of the cam rests on the pusher and compressed the spring to create a force on the small end of the connecting rod, simulating an explosion in the engine, with each rotation of the cam corresponding to the cycle of the piston and crankshaft. When the connecting rod(5) is at the top of dead point, the inertia of the connecting rod and the piston pulls the connecting rod, at this time the cam doesn't touch the pusher and there is no force acting on the piston, the piston doesn't produce force but due to inertial force

on the piston and connecting rod acting on the connecting-rod big end. When the piston reaches the bottom of the dead point, the inertia of the piston and the connecting rod compressed backward, the bearing continues to be affected by the inertia force of the piston and the body of connecting rod

C. Hydraulic system

The oil supplied to the bearing is sucked from the oil tank(21) and passed through the radiator(250) along the oil supply line to the pressure gauge(18) and the flow(19) to determine the oil flow and pressure. Oil through the distributor valve(16) enters to lubricate the bearing. Afterward, oil returns to the path inside the crankshaft to the oil tank(21)

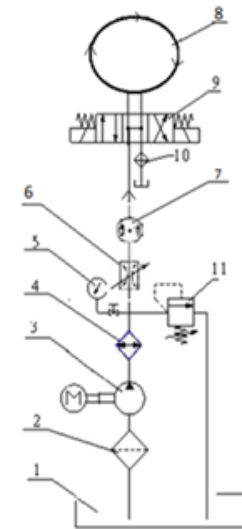


Fig. 3: Hydraulic system

D. Control system

The power of the device is a 3-phase electric motor, with a capacity of 5.5 kW with a rotation speed of 1455rpm. Motor speed control using ABB ACS355-03E-15A6-4 inverter. The experimental device can operate with two models of two modes of control and control with 3 fixed speeds as shown in Figure 4.



Fig. 4: Control system

III. METHOD OF MESUREMENT

A. System for measuring the load acting on the drive

During operation, the load acting on the connecting rod consists of two components (figure 5), the tension/compression force F_x and the bending force F_y . To determine these two

forces, we use strain sensors and connect the bridge circuit, a bridge circuit that measures bending forces. We place the sensor at the position shown in the figure to receive the most accurate force acting on the big end of connecting rod

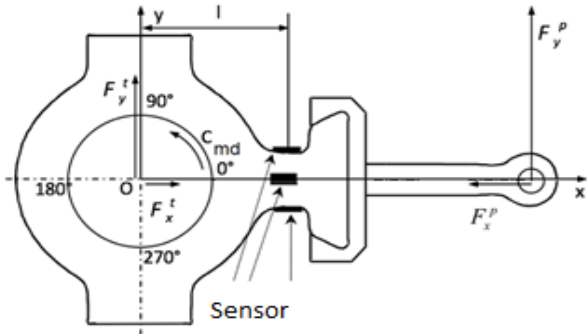


Fig. 5: Diagram force sensor

To measure the compressive force F_x , we use two parallel sensors on the top and bottom of the connecting rod and two sensors not placed on the connecting rod to connect the bridge to circuit. Similarly, to measure the bending force F_y , we use a bridge circuit with 4 sensors glued in parallel on both sides of the connecting rod as shown in Figure 6. The sensors will be connected to the data processor, then the signal is connected with a computer and the measurement results are displayed on Labview

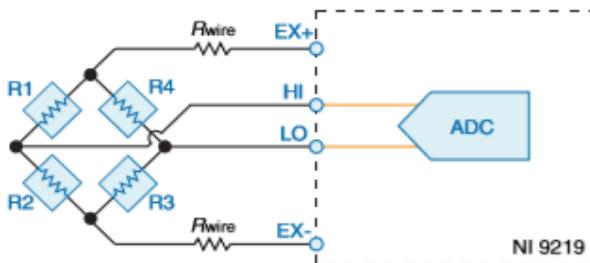


Fig. 6: Principle diagram of load measurement

B. Oil film temperature measuring system

To measure the temperature of the oil film lubrication of the connecting-rod big end bearing, we use the thermocouple type K. The structure of thermocouple consists of two different metal wires that are chemically bonded at one end (hot end) to the other end (cold end). The thermocouple sensor is based on the difference in temperature between the two terminals of the two wires (hot and cold head) different in chemical nature so that there appears electromotive force in the circuit. By measuring the electricity of the electrolyte, we can obtain the corresponding temperature. Thermocouple sensor type K include one wire 0.5 mm, temperature rage -200 oC to 1250 oC

To measure the temperature of the oil film in the connecting-rod big end bearing, the research had used six temperature sensors thermocouple type K which are placed at six positions at angle $0^\circ, 45^\circ, 135^\circ, 180^\circ, 225^\circ, 315^\circ$ of boring. Figure 8 The temperature measurement system is using DAQ hardware to collect analog data from temperature sensors. Thanks to National Instruments Measurement signals are processed and programmed using NI-DAQmx software and display results in LabVIEW software. National Instruments.

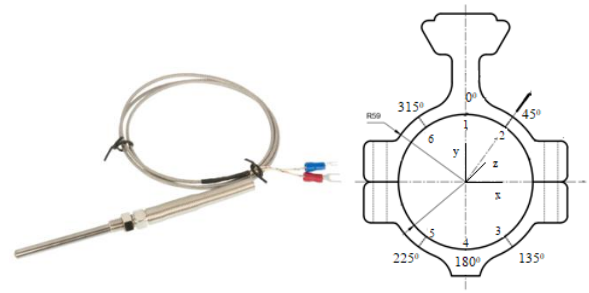


Fig. 7: Structure of thermocouple

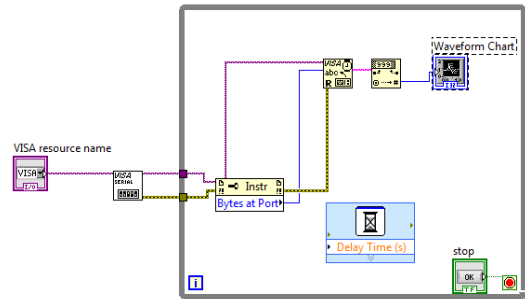


Fig. 8: Signal diagram labview

C. Pressure measuring system

To measure the oil film pressure of the connecting-rod big end, we use the selected KULITE XCQ-062 35BARA resistance sensor. The sensor has a diameter of 1.7 mm, a length of 9.5 mm. Sensor has measuring range $0.7 \div 70 \text{ bar} \div 1000 \text{ Psi}$, max pressure range $2 \div 3$ rated pressure, voltage source $10 \div 12 \text{ VDC}$, operating temperature $-65^\circ\text{F} \div +275^\circ\text{F} (-55^\circ\text{C} \div +135^\circ\text{C})$. The sensor rotates with the shaft, so there is no direct electrical connection between the sensor and the central data processor. One solution is to transmit and receive wireless signals. To solve the problem, we choose RF signal transmission system. The signal of pressure sensor XCQ-062-35BARA is an analog signal.

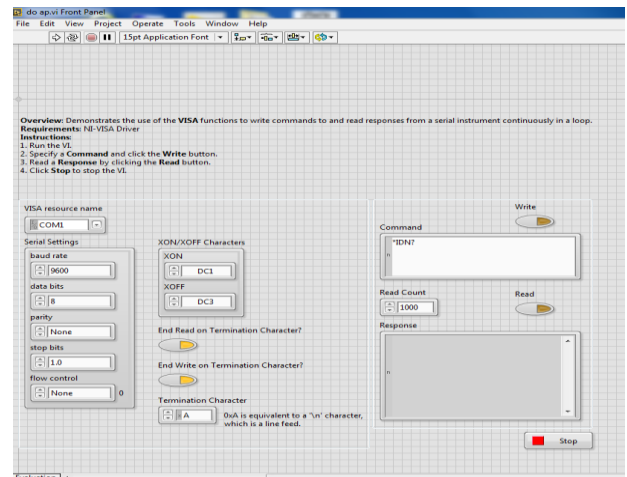


Fig. 9: Pressure of oil film throughout the time according to the Labview software.

The wireless analog signal transmission through the RF transmitter gives a very small measurement value, so the signal of the pressure sensor XCQ-062-35BARA needs to be

amplified and will be converted from an analog signal to a digital signal through a digital converter. The signal receiver sends a signal to the measuring circuit, the signal from the receiver will be transmitted to the computer and the results will be displayed on LabView Figure 9 is the interface to read the oil film pressure signal on LabView

IV. RESULT OF RESEARCH AND SURVEY

TABLE 1: Technical Information oil

Technical Information	Atox 320	Besil F100
Density at 20°C, (g/ml)	0.875	0.97
Viscosity (cSt)	288/352 at 40°C	250/400 at 25°C
Pour point, (°C)	-12	-50
Flash point, (°C)	256	300
Viscosity index	118	101

A. Result of applied force

The force acting on the connecting rod is measured according to the crankshaft rotation during the duty cycle at different speeds. Figure 10 is the pulling/compression force acting on the connecting rod at the speed of 10rpm, the maximum force acting on the rod conveys the greatest value in the region where the simulated explosion occurs, around the corner 360o of the crankshaft. The maximum value of the tension/compression force is 385.25N

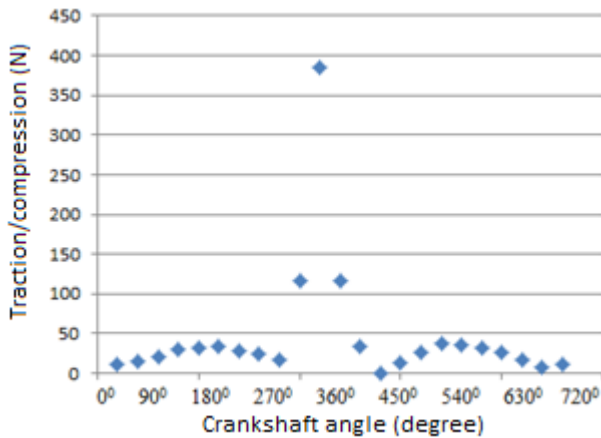


Fig. 10: Traction/compression force acting on the connecting rod at a rotational speed of 100rpm

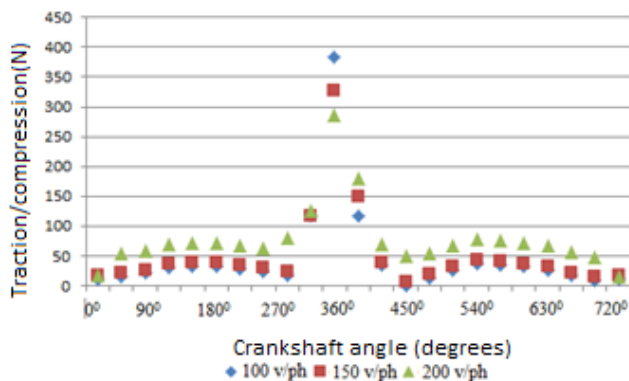


Fig. 11: Traction/compression force acting on the connecting rod according to the crankshaft rotation at different rotational speeds

Figure 11 shows the traction/compression force acting on the connecting rod at the rotational speed of 100 rpm, 150 rpm,

and 200 rpm. We see, when increasing the rotational speed, the maximum force acting on the connecting rod at the time of explosion decreases. This is because the force of inertia increases with increasing rotational speed and in the region where the detonation occurs, the force of inertia is opposite to the simulated air force acting on the connecting rod, so the total force acting on the connecting rod decreases.

B. Test result of pressure measurement

We see, the oil film pressure reaches the maximum value(0.857MPa) at around the angle of 360⁰ of the crankshaft, which is the time of the explosion. At this time, the load acting on the connecting rod is the largest, the oil film thickness reaches the minimum value. The oil film pressure reaches the minimum value(0.152 MPa) at around 0⁰ angle(720⁰) of the crankshaft, the moment the connecting rod is at the top of dead point, corresponding to the minimum load area acting on the connecting rod. Figure 13 is the connecting rod big end pressure at 0⁰ of the connecting rod at rotational speeds from 100 rpm to 200 rpm. It can be seen that the maximum pressure of the oil film decreases as the rotational speed increases. This is consistent with the theory because with increasing speed, the minimum oil film thickness will increase

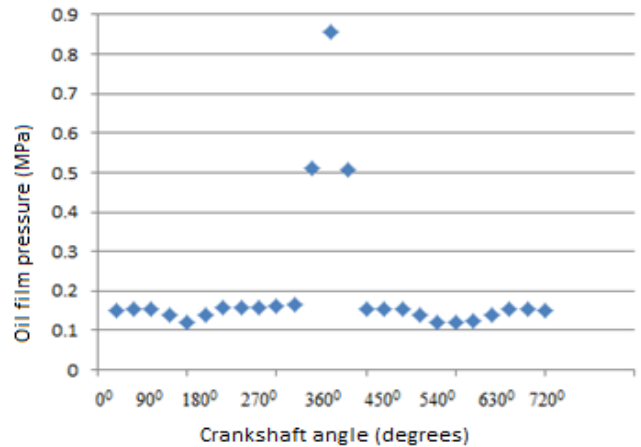


Fig. 12: Oil film pressure according to crankshaft rotation angle at 0o of connecting rod, rotational speed 150rpm

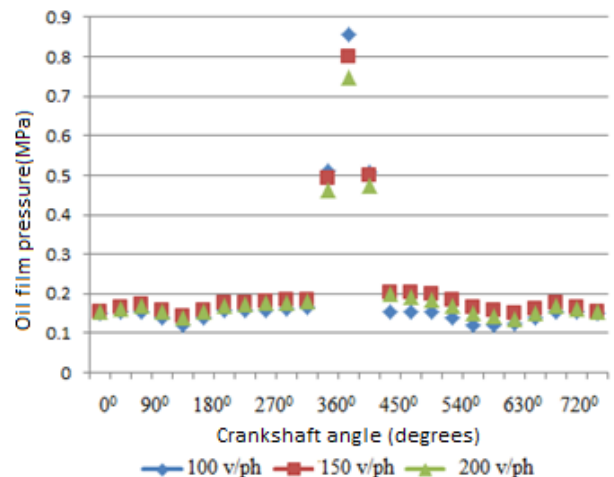


Fig. 13: oil film pressure according to crankshaft rotation angle at 0⁰ of connecting rod at different rotational speeds

C. Test results of temperature measurement

Experiment with BESIL F-100 oil with kinematic viscosity $\mu = 0.135$ Pa.s. Figure 14 shows the temperature range of sensor 1 and sensor 2 being the highest. Sensor 1's temperature reached 27.1987 0C and sensor 2's temperature reached 26.7465 0C because sensor 1's position was at the 0th angle of the connecting rod where the explosion occurred the temperature value at that location was highest.

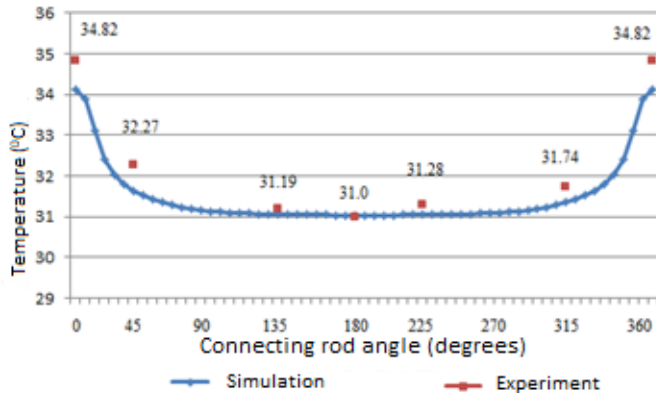


Fig. 14: Comparison of simulation and experimental results of oil film temperature at 100 rpm, crankshaft angle 360°, Besil F100 lubricating oil.

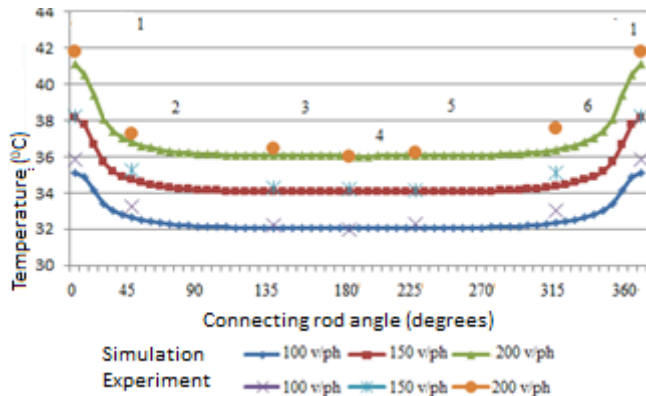


Fig. 15: Comparison of simulation and experimental results of oil film temperature at different speeds, crankshaft angle 360°, Atox 320 lubricating oil when the bearing reaches a steady state.

Figure 14 Comparison of simulation and experimental results of oil film temperature in the bearing at 100 rpm with Besil F100 lubricating oil when the bearing reaches steady state after 2500 cycles and the steady state temperature increases 6⁰C above the input temperature. We see the simulated oil film temperature and experimental oil film are similar, however, there are differences in temperature values at the corner of the connecting rod. The largest oil film temperature difference at the angle 0⁰, 45⁰, 315⁰ of the connecting rod, 34.11⁰C (calculated result) and The largest oil film temperature difference at the angles 0⁰, 45⁰ và 315⁰ of the connecting rod, 34.11⁰C (calculated result) and 34.82⁰C (experimental result) at the 0⁰ angle of the connecting rod,, 31.6⁰C (calculated result) and 32.7⁰C (experimental result) at 45⁰ angle of connecting rod, 31.34⁰C (calculated result) and 31.74⁰C (experimental result) at 315⁰ angle of connecting rod. At the 180⁰ angle of the connecting rod, there is almost no difference. At the angle of

225⁰ of the connecting rod, the difference is not large, 31.04⁰C (calculated result) và 31.28⁰C (experimental result). Errors due to numerical simulation programs don't take into account the lubrication effects and may also be due to errors in measurements.

Similar to Besil F100, when lubricating with Atox 320, the oil film temperature also has the same rule of difference between the calculated and experimental results (Figure 15). The oil film temperature are determined when the bearing has stabilized. With speeds of 100 rpm, 150 rpm and 200 rpm, the spectrum operates stably after 1500, 2000, 2500 cycles, respectively. At the lowest speed (100 vg/ph), the difference is greatest at positions 0⁰, 45⁰ và 315⁰ of the connecting rod. When the rotational speed is higher, 150 rpm and 200 rpm, the calculated and experimental oil film temperature difference decreases, except at 315⁰ angle of connecting rod. From the experimental results, we can see that the temperature field of the lubricating oil film in the connecting-rod big end has similar temperature. As the rotation speed increases, the temperature rise also increases, the faster the rotation speed, the higher the temperature rises. Maximum temperature at angle 0⁰ (360⁰) of connecting rod, lowest temperature at 180⁰ angle position of connecting rod.

V. CONCLUSION

This research presents working principle and structure of experimental equipment. Typical assemblies are calculated and manufactured such as connecting rods, load-forming mechanism assemblies, connecting rod assemblies and hydraulic systems, load measuring systems acting on connecting rods, pressure measuring systems and heat measuring systems. oil film level in the connecting rod big head. The connecting rod bearing lubricating oil film temperature is measured at six positions in the circumference and at the center section of the bearing in the longitudinal direction via "thermocouple type K" temperature sensors. The pressure of the connecting rod bearing lubricating oil is determined through the XCQ-062 pressure sensor located on the shaft of the bearing. The load applied to the connecting rod is measured by a strain gauge connected to the bridge circuit. The experimental equipment operates stably, and the measurement results are tested with standard measuring devices. The experimental equipment can be applied to research on lubrication as well as internal combustion engines in experimental research activities or testing numerical simulation results.

REFERENCES

- [1] Reddi, M.M, 1969 "Finite Element Solution of the Incompressible Lubrication problem." ASME, Journal of Lubrication Technology, pp.262 – 270
- [2] Oh, K.P., Huebner, K.H., 1973 "Solution of the Elastohydrodynamic Finite Journal Bearing Problem.", ASME Journal of Lubrication Technology, Vol. 3, pp.342 – 352
- [3] Fantino B., FreneJ, Du Parquet J (1979) "Elastic connecting-rod bearing with piezoviscous lubrication: Analysis of the steady-state characteristics", Transaction of the ASME, Journal of Lubrication Technology, vol. 101, p. 190-200.
- [4] Pierre-Eugene, J., Frêne, J., Fantino, B., Roussel, G., Du Parquet, J., (1983) "Theory and Experiments on Elastic Connecting-Rod Bearings Under Steady State Conditions.", 9th Leeds-Lyon Symposium on

- Tribology, Leeds, Grande-Bretagne.
- [5] H. Shahmohamadi., 2014, "Big End Bearing Losses with Thermal Cavitation Flow Under Cylinder Deactivation". *Tribol Lett* (2015) 57:2
- [6] H. Chamani., 2015, "Thermo-elasto-hydrodynamic (TEHD) analysis of oil film lubrication in big end bearing of a diesel engine". Vol. 5, No. 1, Aut.-Win. 2015-16.
- [7] Norbert Lorenz., 2017, "Thermal analysis of hydrodynamic lubricated journal bearings in internal combustion engines". *Proc IMechE Part K: J Multi-body Dynamics*.
- [8] H. Shahmohamadi, R. Rahmani, H. Rahnejat, C. P. Garner , D. Dowson(2015) "Big End Bearing Losses with Thermal Cavitation Flow Under Cylinder Deactivation.", *Tribol Lett* (2015) 57:2
- [9] N. Morris, M. Mohammadpour, R. Rahmani, P.M. Johns-Rahnejat, H. Rahnejat and D. Dowson (2018) "*Effect of Cylinder Deactivation on tribological performance of pit-tông compression ring and connecting rod bearing.*", *Tribology International* (2018), doi: 10.1016/j.triboint.2017.12.045.
- [10] T.T.H.Tran (2018), "*A solution for creating the simulating load on connecting-rod in the experimental device for lubrication condition of the connecting-rod big end bearing* ", *journal of science and technology*, september, 2018 .